Supplement of

Contributions of Fine and Coarse Particles to Light Absorption at an Urban Traffic Site during Street Dust Season

Luis M. F. Barreira et al.

Correspondence to: Luis M. F. Barreira (luis.barreira@fmi.fi)

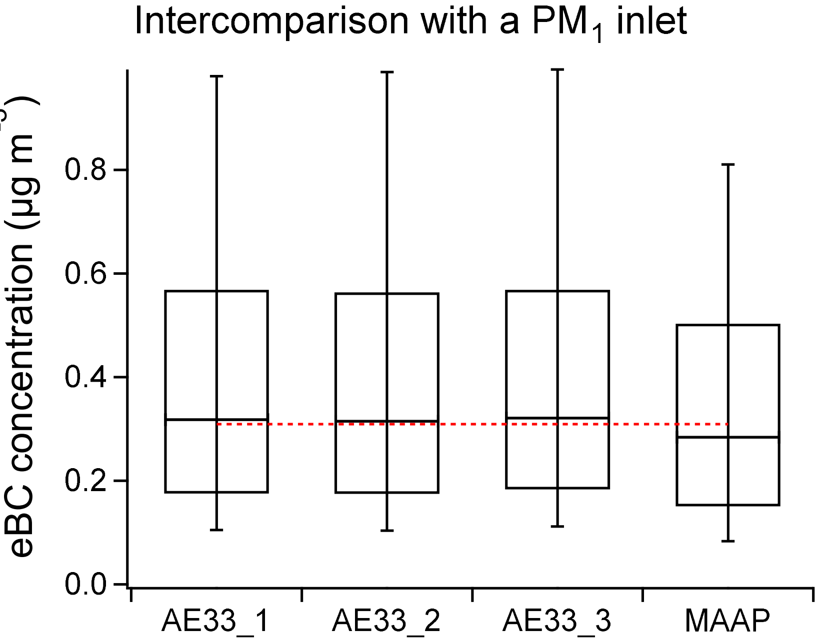

Figure S1: Intercomparison of equivalent black carbon (eBC) measured by different optical instruments. The three AE33 aethalometers deployed throughout the urban campaign and one MAAP were used: AE33_1 measured PM_1, AE33_2 measured $PM_{2.5}$, AE33_3 measured $PM_{7.2}$, and the MAAP measured PM_1 as a reference. The mean eBC concentration across all instruments is indicated by the red dotted line.

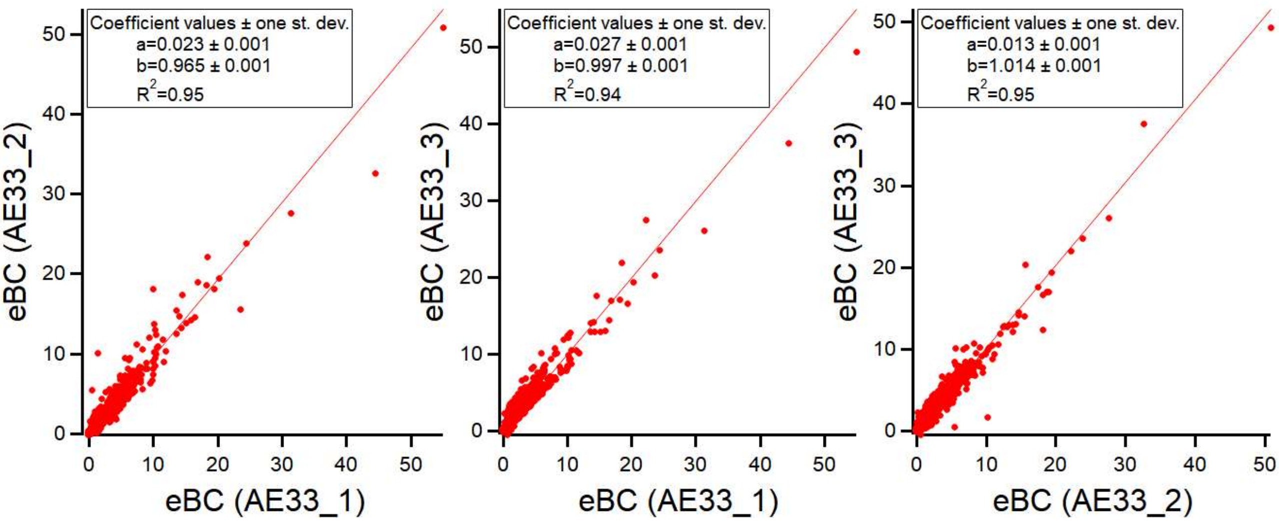

Figure S2: Pairwise comparison of equivalent black carbon (eBC) concentrations measured in PM_1 by three AE33 instruments (AE33_1, AE33_2, and AE33_3), used to measure light absorption in PM_1, $PM_{2.5}$, and $PM_{7.2}$, respectively. Scatter plots show eBC from AE33_2 versus AE33_1, AE33_3 versus AE33_1, and AE33_3 versus AE33_2.

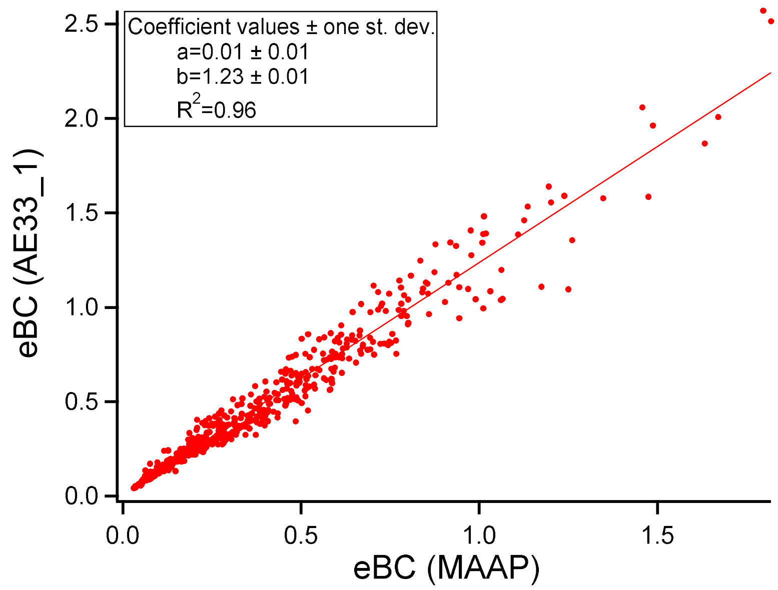

Figure S3: Comparison of hourly-averaged equivalent black carbon (eBC) concentrations measured in PM_1 by the AE33 aethalometer (AE33_1) and MAAP.

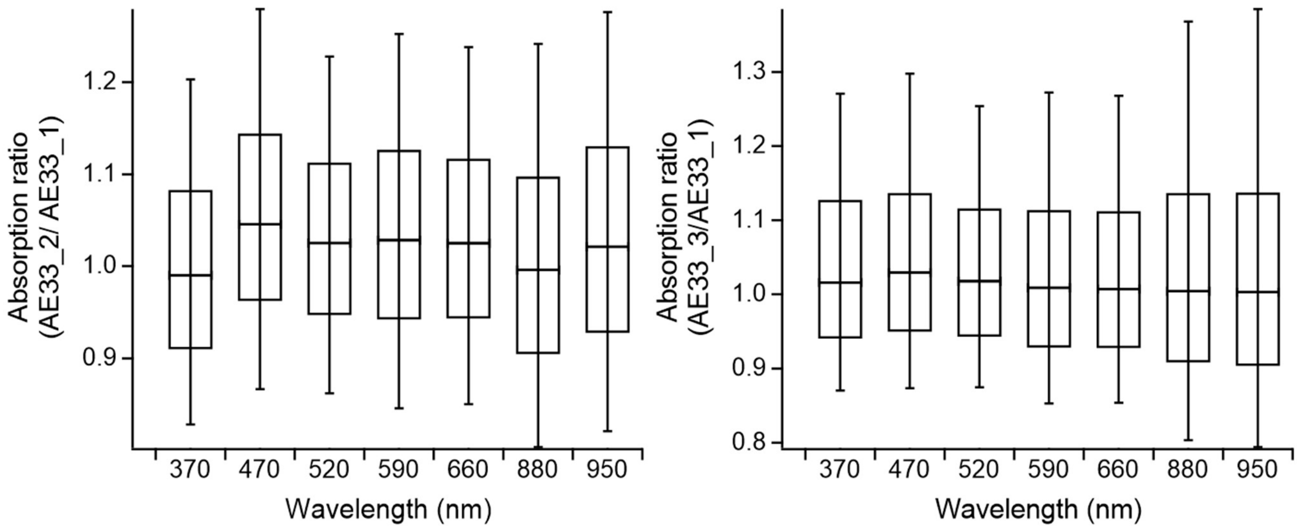

Figure S4: Ratios of light absorption measured by the AE33 equipped with $PM_{2.5}$ and $PM_{7.2}$ inlets relative to the AE33 operating with a PM_1 inlet. The left panel shows the absorption ratio of AE33_2 to AE33_1, while the right panel shows the ratio of AE33_3 to AE33_1.

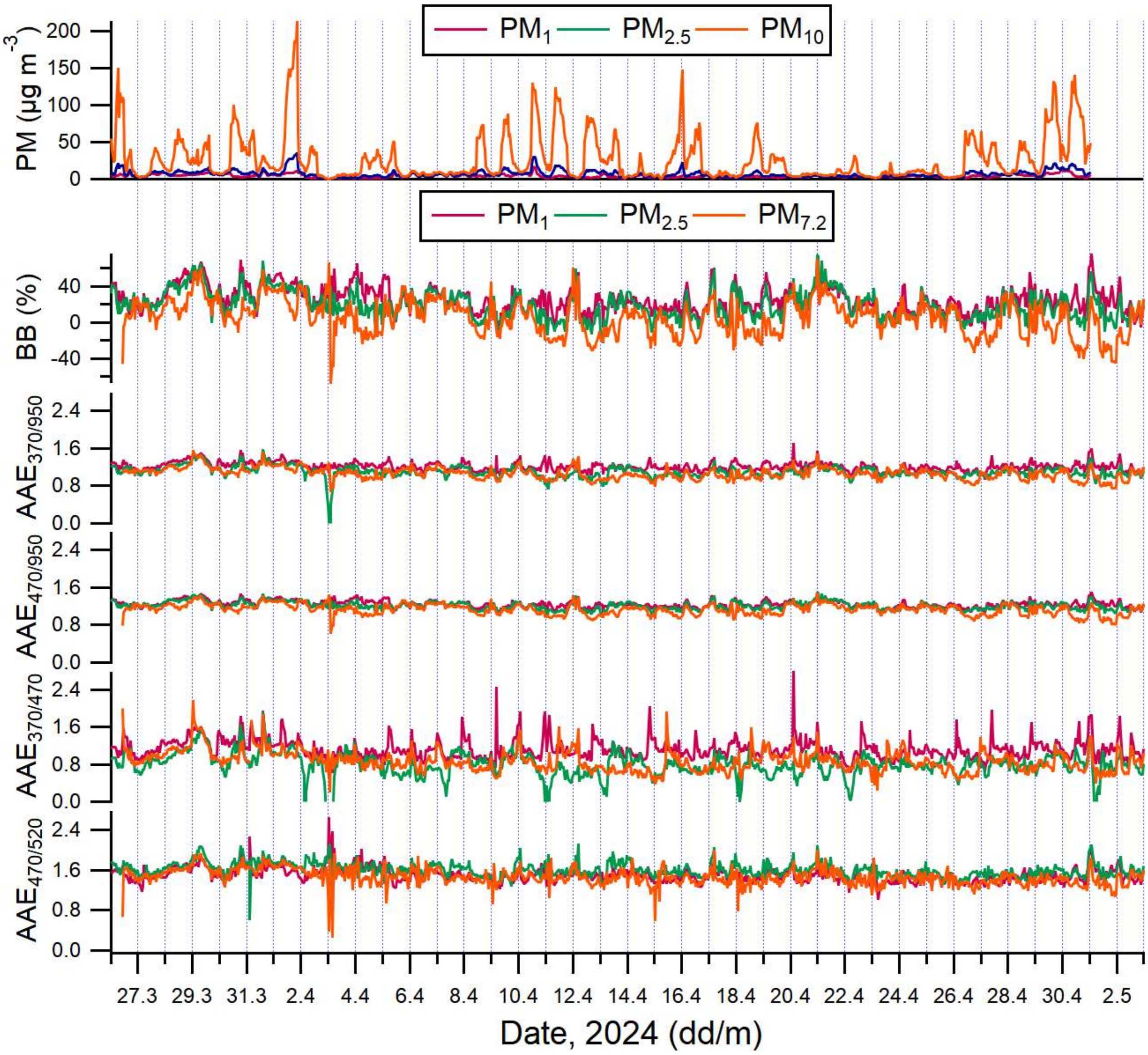

Figure S5: Time series of the Absorption Ångström Exponent (AAE), calculated for different wavelength pairs (370/470, 470/950, 370/950, and 470/520 nm), and of BB percentage in PM_1 (brown), $PM_{2.5}$ (blue), and $PM_{7.2}$ (orange) during the measurement campaign. For comparison, the top panel shows the total PM mass concentration for PM_1, $PM_{2.5}$, and PM_{10}, using the same colour scheme.

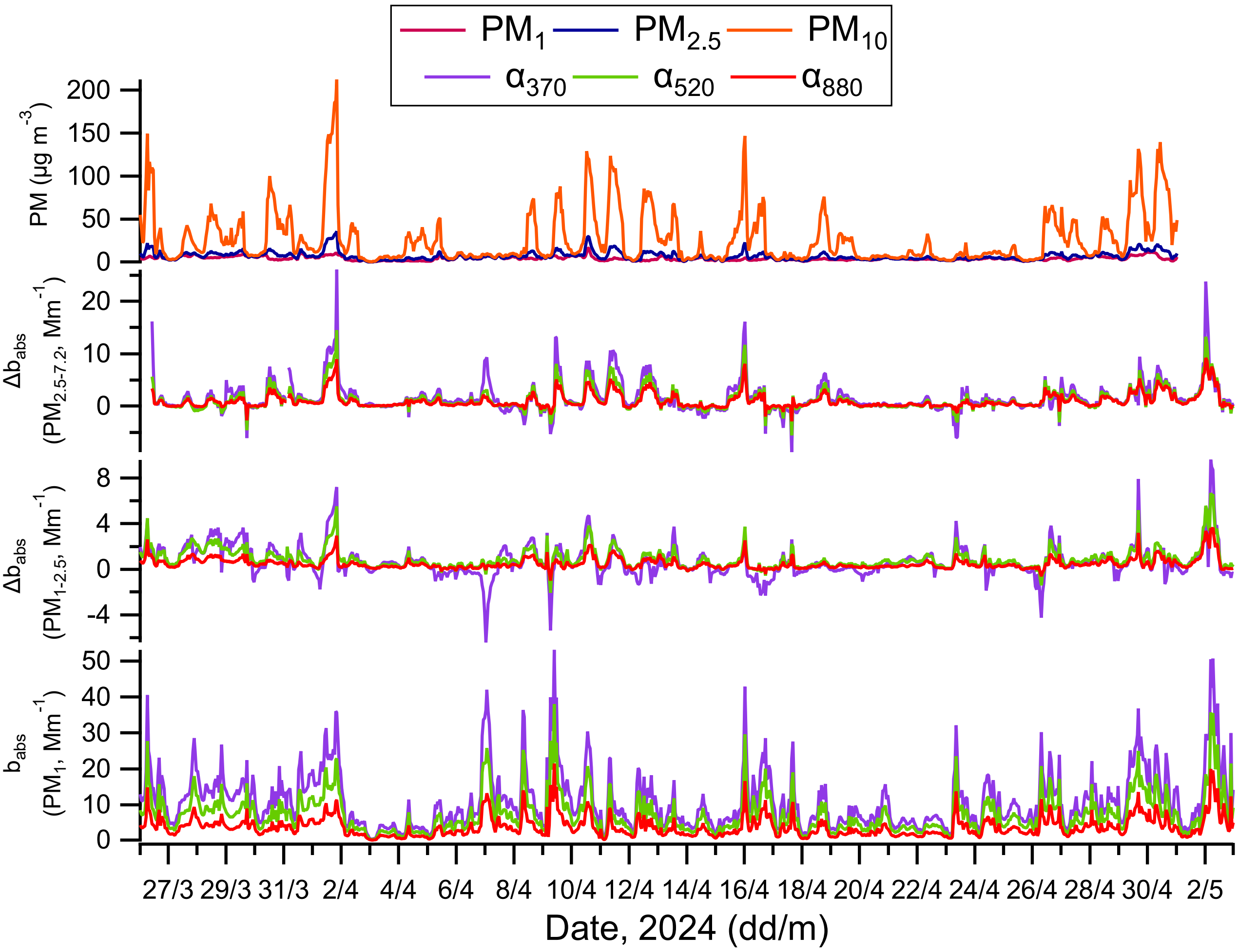

Figure S6: Time series of hourly mean absorption coefficients for different PM size fractions (the stacked panels show PM_1 at the bottom, $PM_{1-2.5}$ in the middle lower panel, and $PM_{2.5-7.2}$ in the upper lower panel; purple = 370nm, green = 520 nm, and red = 880 nm). For comparison, the top panel shows hourly mean total PM mass concentration in PM_1 (brown), $PM_{2.5}$ (blue), and PM_{10} (orange).

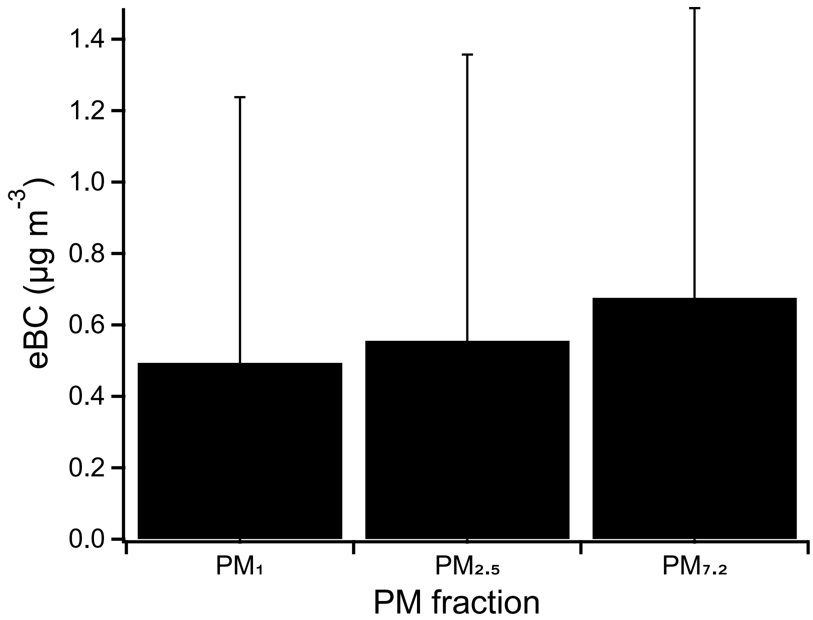

Figure S7: Campaign-averaged concentrations and standard deviations of equivalent black carbon (eBC) in PM_1, $PM_{2.5}$, and $PM_{7.2}$ fractions (expressed in µg m^{-3}).

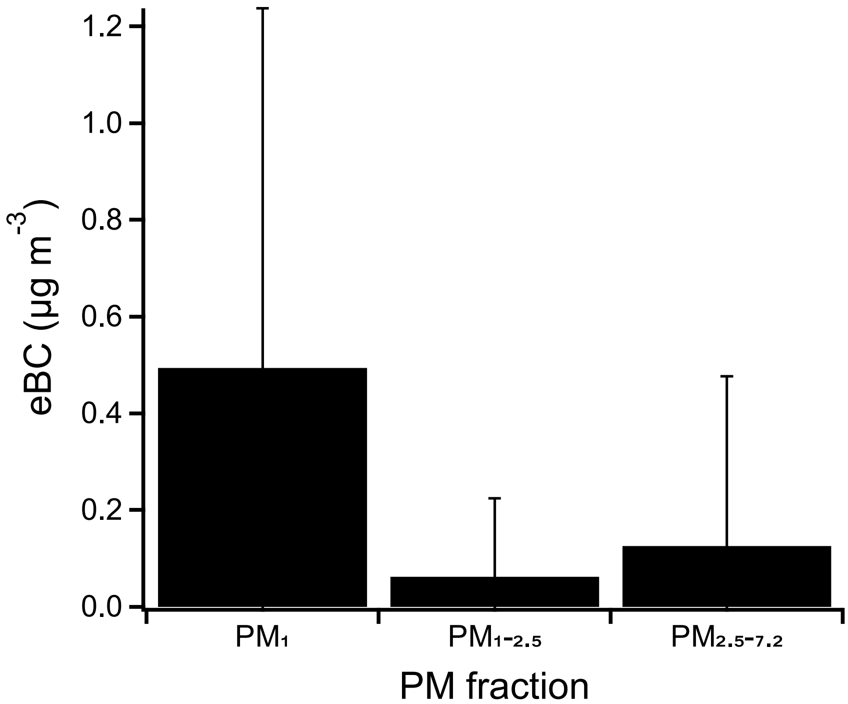

Figure S8: Campaign-averaged concentrations of equivalent black carbon (eBC) in the PM_1, $PM_{1-2.5}$, and $PM_{2.5-7.2}$ fractions (expressed in µg m^{-3}).

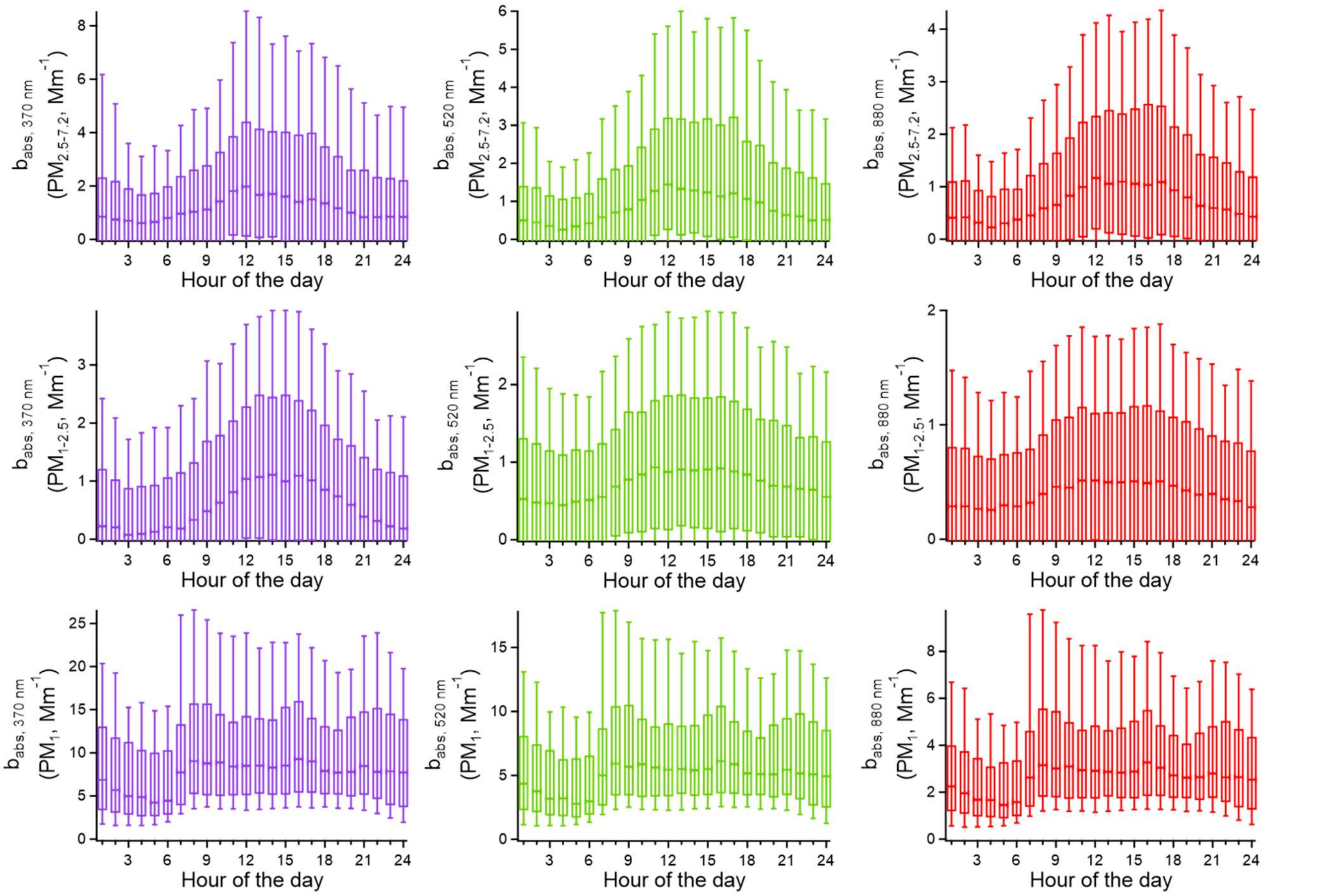

Figure S9: Diurnal variation of absorption coefficients for different particle size fractions. Panels show absorption in PM_1 (bottom), $PM_{1-2.5}$ (middle), and $PM_{2.5-7.2}$ (top) at 370 nm (purple), 520 nm (green), and 880 nm (red). In each box, the mid-line represents the median, box edges indicate the 25th and 75th percentiles, and whiskers extend from the 10th to 90th percentiles. The y-axis was set to zero since absorption differences are inherently positive and, therefore, any small negative values that may occur are due to instrument noise or minor data processing variability which are not physically meaningful.

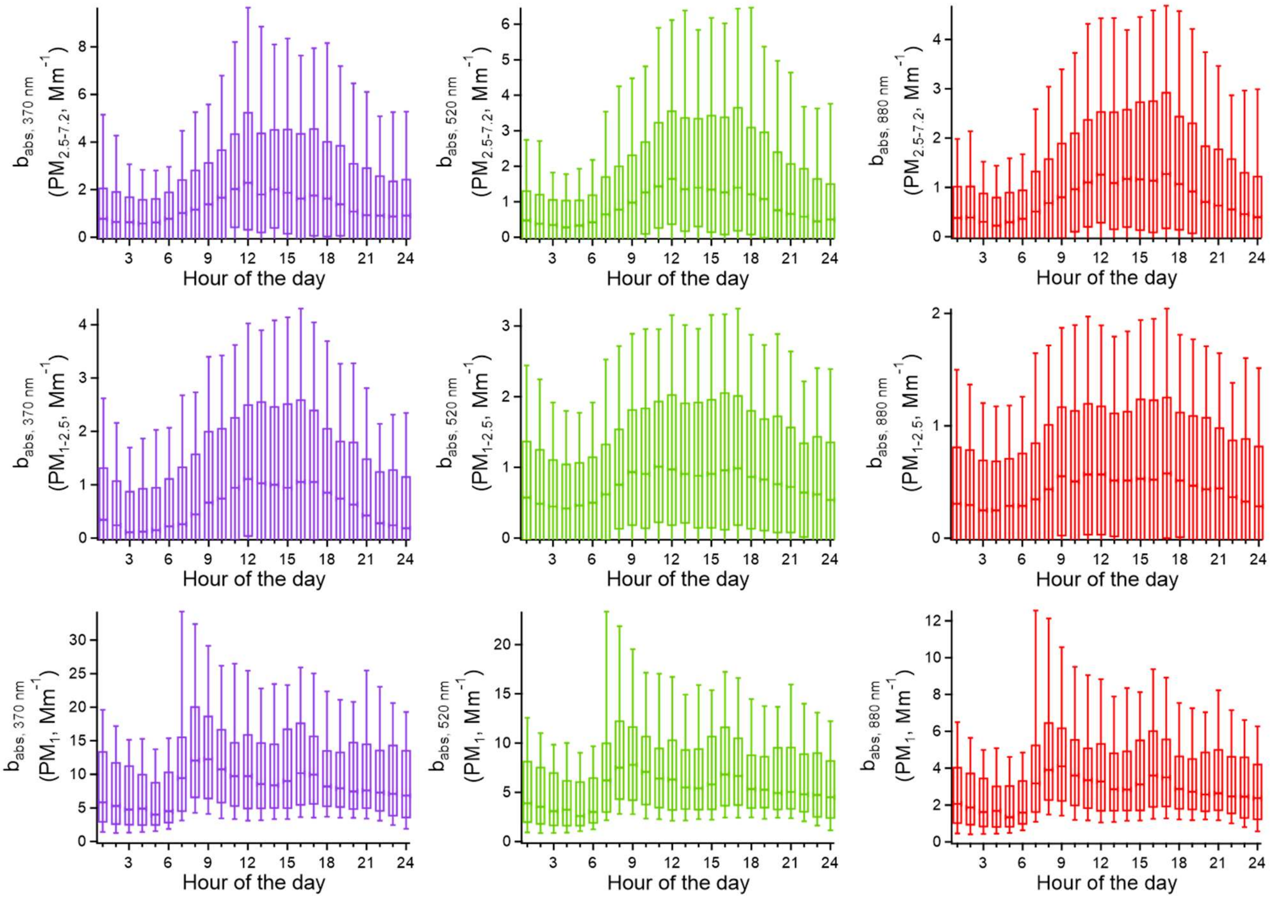

Figure S10: Diurnal variation of absorption coefficients for different particle size fractions during weekdays. Panels show absorption in PM_1 (bottom), $PM_{1-2.5}$ (middle), and $PM_{2.5-7.2}$ (top) at 370 nm (purple), 520 nm (green), and 880 nm (red). In each box, the mid-line represents the median, box edges indicate the 25th and 75th percentiles, and whiskers extend from the 10th to 90th percentiles. The y-axis was set to zero since absorption differences are inherently positive and, therefore, any small negative values that may occur are due to instrument noise or minor data processing variability which are not physically meaningful.

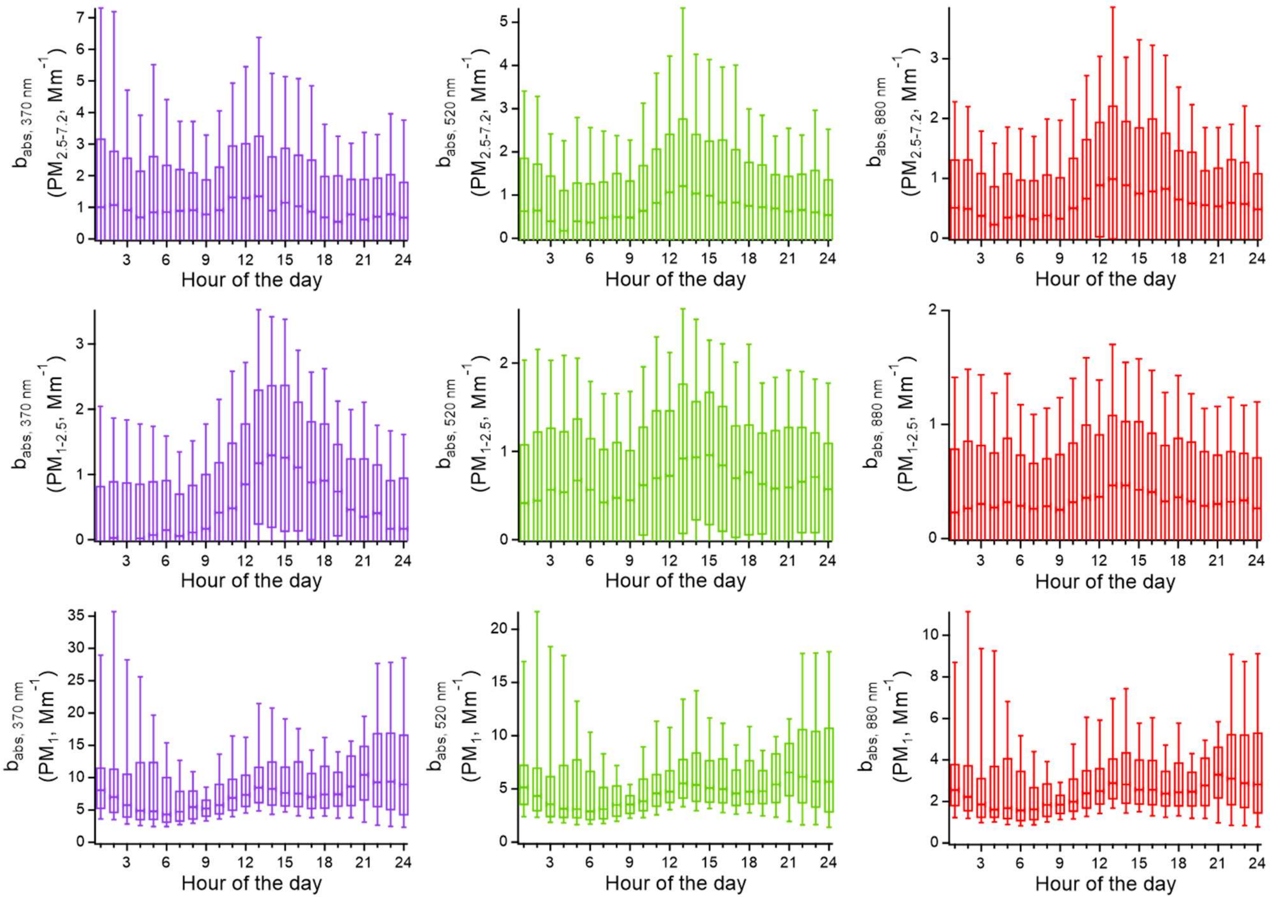

Figure S11: Diurnal variation of absorption coefficients for different particle size fractions during weekends. Panels show absorption in PM_1 (bottom), $PM_{1-2.5}$ (middle), and $PM_{2.5-7.2}$ (top) at 370 nm (purple), 520 nm (green), and 880 nm (red). In each box, the mid-line represents the median, box edges indicate the 25^{th} and 75^{th} percentiles, and whiskers extend from the 10^{th} to 90^{th} percentiles. The y-axis was set to zero since absorption differences are inherently positive and, therefore, any small negative values that may occur are due to instrument noise or minor data processing variability which are not physically meaningful.

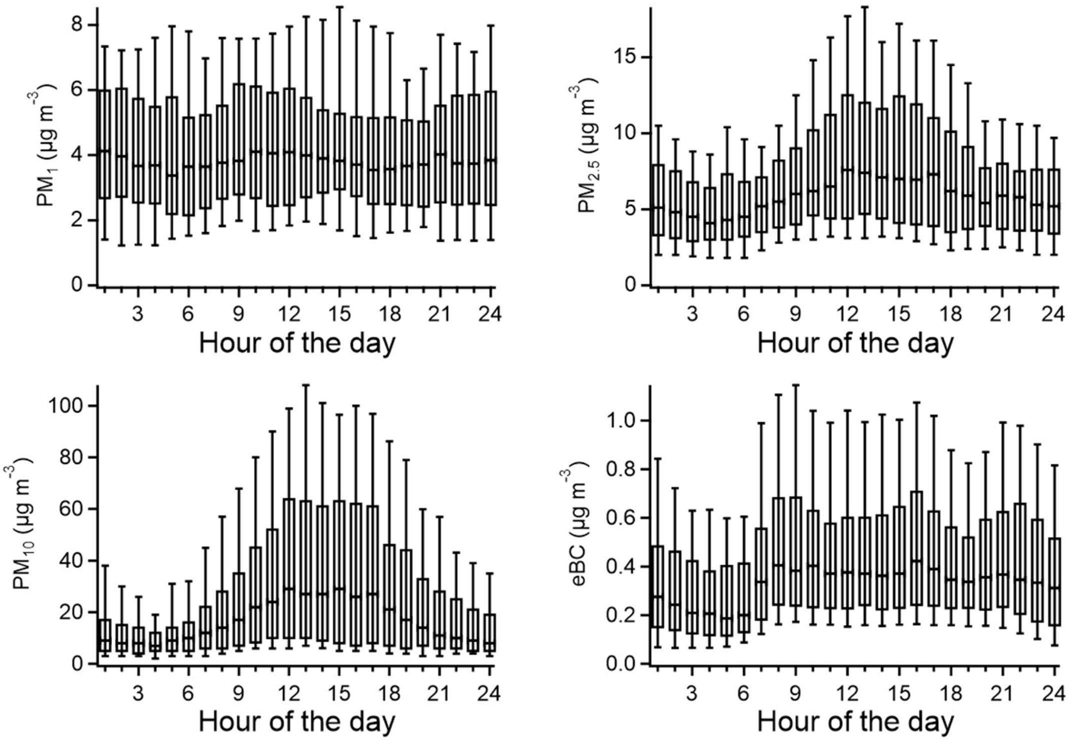

Figure S12: Diurnal variation of particle concentrations: PM_1 (top left), $PM_{2.5}$ (top right), PM_{10} (bottom left), and black carbon in PM_1 (eBC, bottom right). In each box, the mid-line represents the median, the box edges indicate the 25th and 75th percentiles, and whiskers extend from the 10th to 90th percentiles.

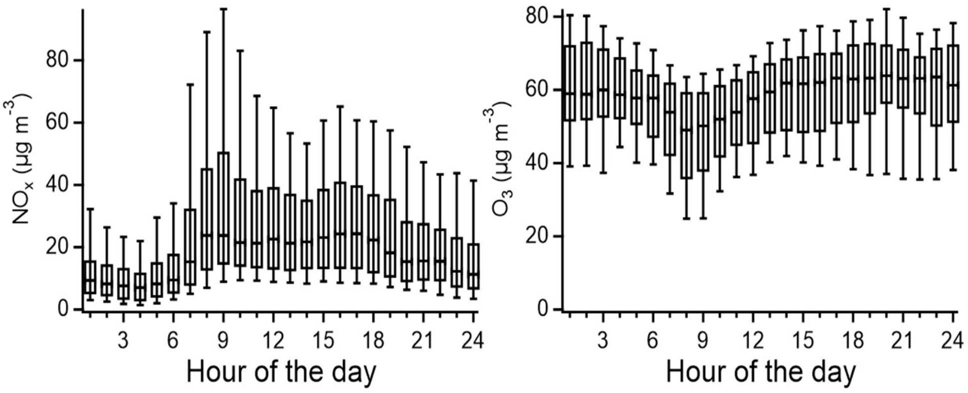

Figure S13: Diurnal variation of NO_x (left) and O_3 (right) concentrations (in µg m^{-3}). In each box, the mid-line represents the median, the box edges indicate the 25th and 75th percentiles, and whiskers extend from the 10th to 90th percentiles.

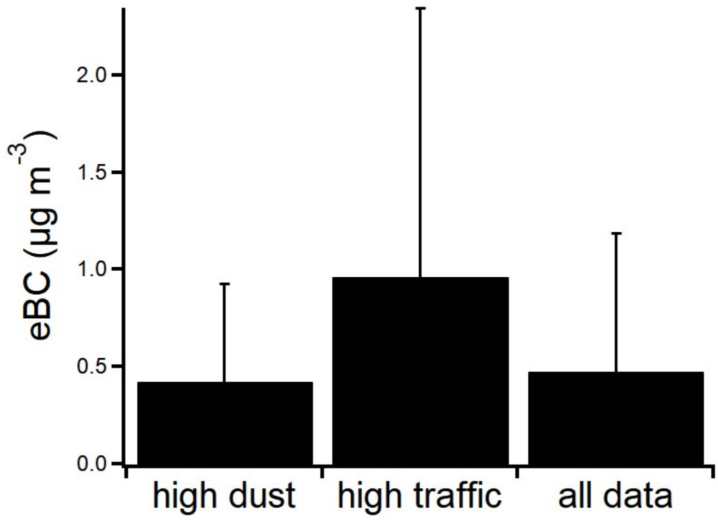

Figure S14: Concentrations of eBC averaged over the entire campaign under different conditions: high PM_{10}: ($PM_{10} \geq 75^{th}$ percentile and $NO_x \leq 50^{th}$ percentile); high traffic: ($PM_{10} \leq 50^{th}$ percentile and $NO_x \geq 75^{th}$ percentile); and all data. The error bars correspond to standard deviations.

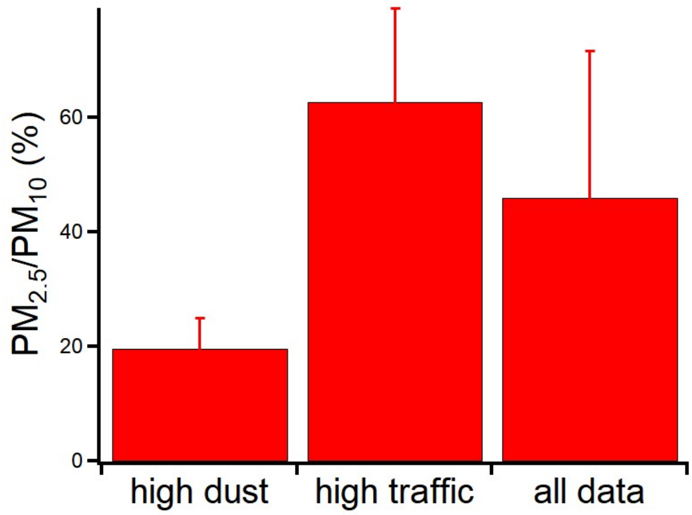

Figure S15: Average fraction of $PM_{2.5}$ absorption to absorption in PM_{10} over the entire campaign under different conditions: high PM_{10}: ($PM_{10} \geq 75^{th}$ percentile and $NO_x \leq 50^{th}$ percentile); high traffic: ($PM_{10} \leq 50^{th}$ percentile and $NO_x \geq 75^{th}$ percentile); and all data. The error bars correspond to standard deviations.

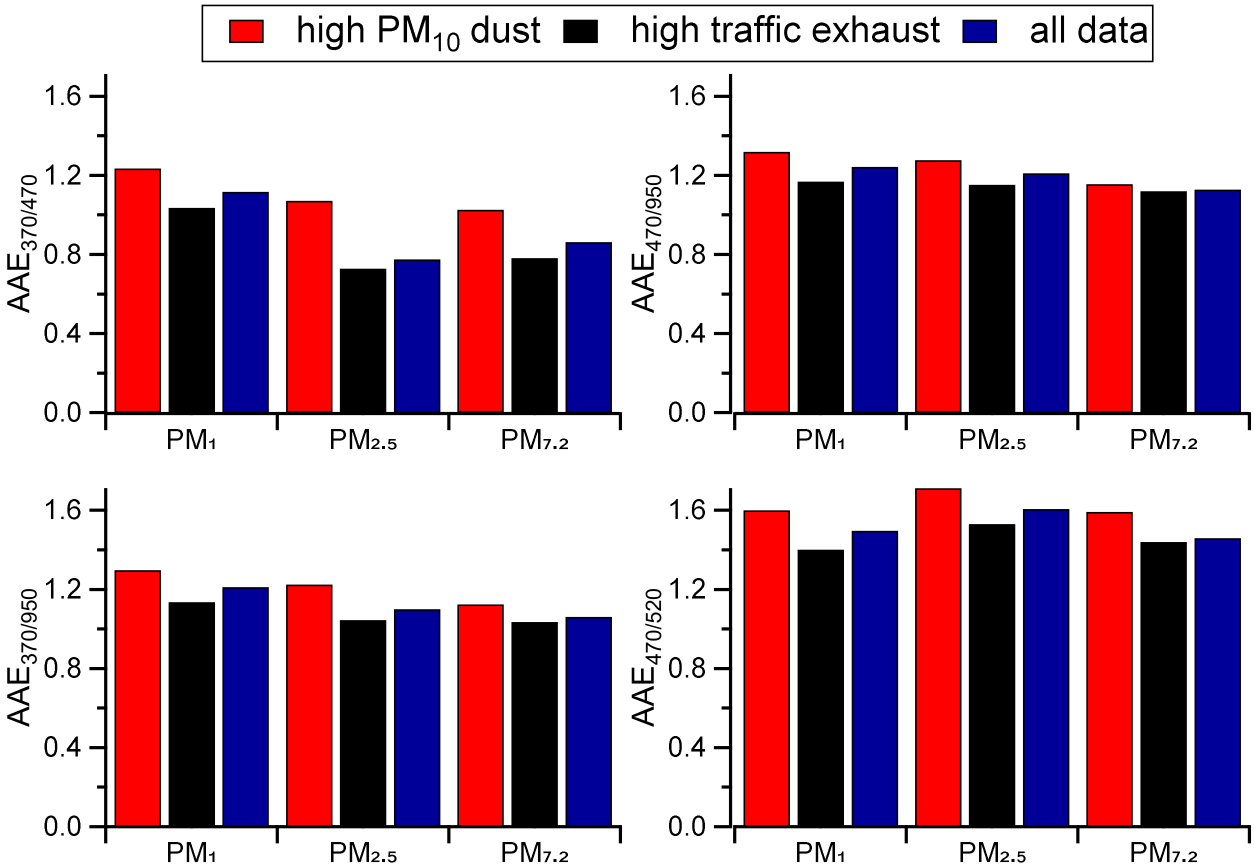

Figure S16: Absorption Ångström Exponent (AAE) values calculated for wavelength pairs $AAE_{370/470}$, $AAE_{470/950}$, $AAE_{370/950}$, and $AAE_{470/520}$ for PM_1, $PM_{2.5}$, and $PM_{7.2}$ under different pollution conditions: high PM_{10} dust episodes (red; $PM_{10} \geq 75^{th}$ percentile and $NO_x \leq 50^{th}$ percentile), high traffic exhaust conditions (black; $PM_{10} \leq 50^{th}$ percentile and $NO_x \geq 75^{th}$ percentile), and all data combined (blue).

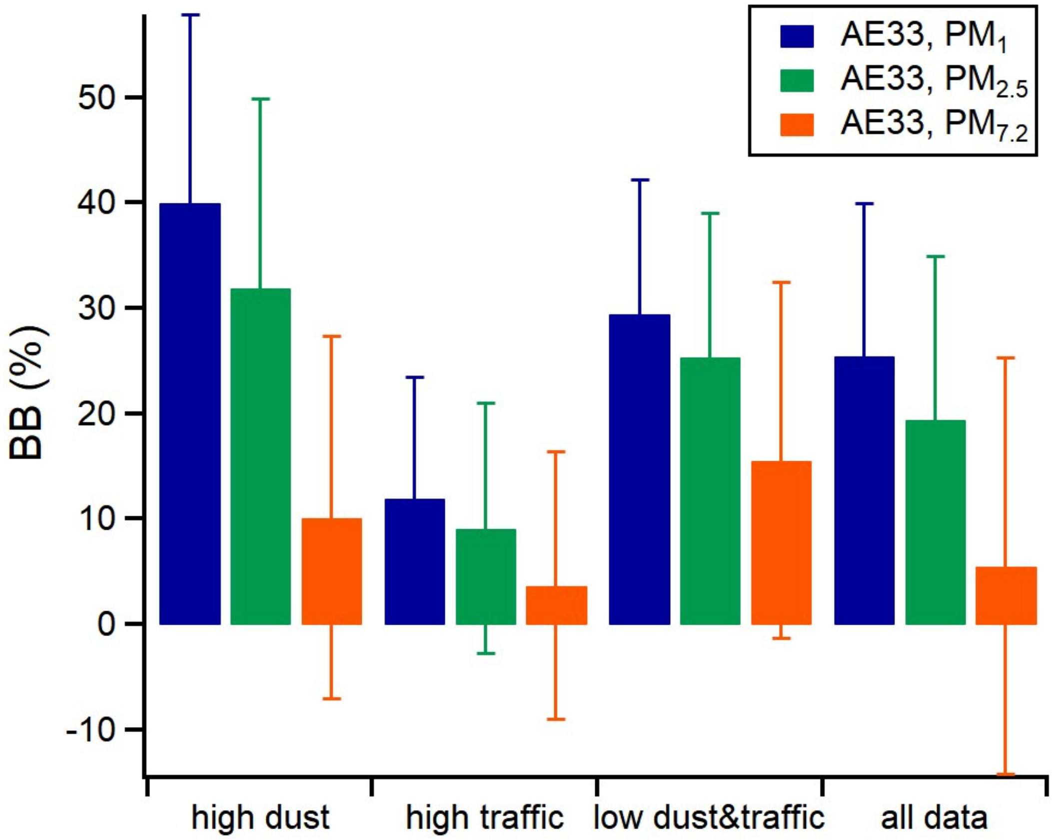

Figure S17: Hourly-averaged BB (%) calculated for PM_1, $PM_{2.5}$, and $PM_{7.2}$ under different pollution conditions: high PM_{10} dust episodes (red; $PM_{10} \geq 75^{th}$ percentile and $NO_x \leq 50^{th}$ percentile), high traffic exhaust conditions (black; $PM_{10} \leq 50^{th}$ percentile and $NO_x \geq 75^{th}$ percentile), low dust and traffic (red; $PM_{10} \leq 50^{th}$ percentile and $NO_x \leq 50^{th}$ percentile) and all data combined (blue).

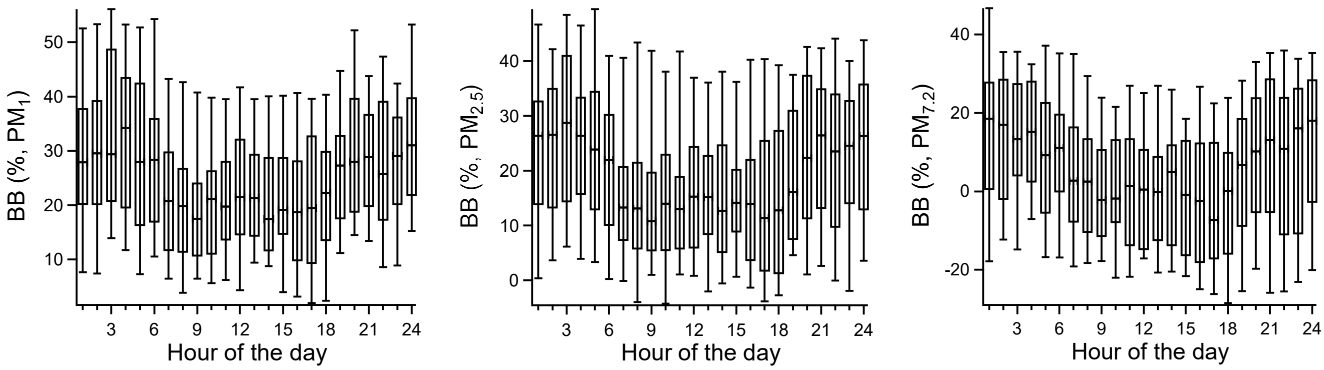

Figure S18: Diurnal variation of BB percentage in PM_1 (left), $PM_{2.5}$ (middle), and $PM_{7.2}$ (right). In each box, the mid-line represents the median, the box edges indicate the 25th and 75th percentiles, and whiskers extend from the 10th to 90th percentiles.

95

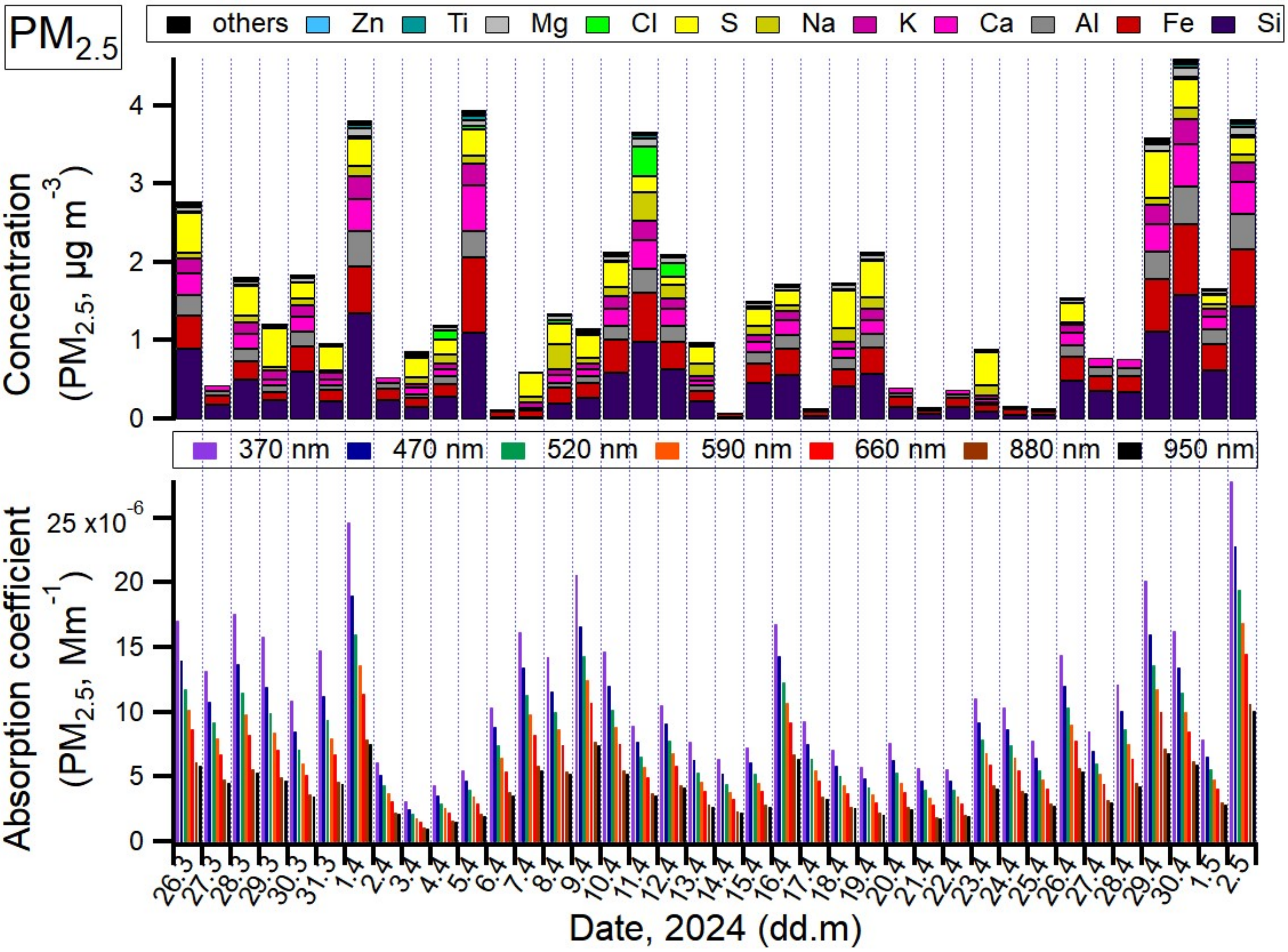

Figure S19: Time series of daily-averaged $PM_{2.5}$ absorption coefficients, measured by the AE33 aethalometer at seven wavelengths (bottom panel), and of elemental concentrations in $PM_{2.5}$ obtained from XRF analysis of 24-h filter samples (top panel).